Saturated Water Storage in Shallow Perched Aquifer With Evapotranspiration From the Phreatic Surface and Unsaturated Lacunae: the Saint-Venant Theory Revisited

F. G. Avkhadiev[1] and A. R. Kacimov[2]

[1]Department of Function Theory and Approximations

Lobachevsky Institute of Mathematics and Mechanics, Kazan Federal University, Kremlevskaya str., 35, 420008, Kazan, Russia,

ORCID: 0000-0001-6927-7102

Emails: avkhadiev47@mail.ru

[2]Department of Soils, Water and Agricultural Engineering, Sultan Qaboos University, Oman

ORCID ID: 0000-0003-2543-3219

Emails: anvar@squ.edu.om,

akacimov@gmail.com

Technical Note

Short title for running head: Perched Aquifer With Evapotranspiration

Submitted to Water Resources Research (Wiley)
on June 29, 2020 as manuscript …
first set of referees comments received on …, 2020;
first revised version submitted: on …;
second set of referees comments received on …;
second revised version submitted: on … ;
accepted:.... rejected: .....

Address for correspondence:
Prof. Kacimov A.R., Department of Soils, Water and Agricultural Engineering
Sultan Qaboos University Al-Khod 123, PO Box 34 Sultanate of Oman
Tel (968) 24141-201 Fax (968) 24413-418
Emails: anvar@squ.edu.om; akacimov@gmail.com
Omani page:
https://www.squ.edu.om/agr/Academics/Departments/Soil-Water-and-Agricultural-Engineering

Abstract. Two models are compared for Darcian flows in a vadose zone and shallow unconfined aquifer with an intensive evapotranspiration, common for hyperarid climates. An analytical 2-D Dupuit-Forchheimer approximation, in which the vadose zone is considered as a "distributed sink" (similar to a standard "distributed source" which models recharge to the water table in humid climates), is collated with HYDRUS3D. In a planar domain, a vertically-averaged flow from a constant piezometric head contour (seepage from ditches or trenches) is studied and integral criteria (the volume of the saturated zone and the area of unsaturated lacuna) are either evaluated or estimated by the Pòlya and Szegö isoperimetric inequalities. Mixed BVPs for Richards' equation in cylindrical domains are numerically solved and give the pressure head, moisture content, and velocity fields, streamlines and criteria. Implicaitons for urban hydrology and ecohydrology of water logged drylands are discussed.

Keywords. Dupuit-Forchheimer model for unconfined aquifer; evaporation from a phreatic surface; HYDRUS-3D simulations; conformal radius and Poincaré metric; isoperimetric inequalities

1. Introduction

Shallow perched aquifers subtanded and sustained by caliche (petrocalcic horizons) or other low-permeable (e.g. gypsic) layers are common for arid and semi-arid regions, where evapotranspiration and human abstraction from dug wells are important components of hydrologic balances, with applicaitns to ecohydrology, MAR, and rural water supply (see e.g. Hamutoko et al., 2019, Niswonger and Fogg, 2008, Villeneuve et al., 2015). Groudnwater and soil moisture motion in these aquifers and thin vadose zone above the water table is modeled both numerically and analytically.

Dirichlet and mixed boundary value problems (hereafter, BVPs) to the Poisson PDE are solved for phreatic, vertically (*Z*-coordinate in Fig.2) averaged Darcian flows in porous (soil, rock) volumes (Aravin and Numerov, 1953, Haitjema, 1995, Polubarinova-Kochina,1962, Strack, 2017 a,b, Zijl et al., 2017). A horizontal cross-section (aerial view) of such a volume is shown in Fig.1a, where D is a planar flow domain and G is its external boundary. Vertical cross-sections are shown in Fig.2. Examples of hydrological prototypes are:

a) in Holland, a rectangular D represents a cropfield bounded by four drainage ditches (G), the water level in which is constant; for a typical dyad (a,h_0) ⌴ (tens of meters, tens of cm);

b) in Oman, the Muscat International Airport is bounded by a shallow trench (see the Photogallery), and (a,h_0) ⌴ (hundreds of meters, tens of cm).

In humid climates (like Holland), a gross-recharge (infiltration) to the aquifer from a vadose zone takes place on a hydrologically-annual time scale and, consequently, the RHS of the Poisson equation, ε, is a negative function of two planar coordinates, x and y. Physically, accretion results in

groundwater mounds whose summits hydraulically command the regional discahrge zones (the curve G in Fig.1, see e.g. Youngs, 1990). Analytical and numerical solutions to these BVPs are applied to groundwater hydrology, agricultural and geotechncial engineering, geomorphology, among others (see e.g. Coffey and Shaw, 2017, Cohen and Rothman, 2017, Haitjema, 1995, Kacimov et al. 2016, 2017a,b, 2020 a, McDonald, 2020, Strack, 2017a). If wells are pumped in D, the mound is drained with a near-well drawdown of the water table. In other words, if $\varepsilon(x,y)$ changes its sign in D, then minima and maxima on the water table emerge (see e.g. Mahdavi, 2020, Strack, 2017a, Fig.2.3.3).

In Oman and other Gulf coutnries, where the aridity index > 20, shallow unconfined aquifers often evaporate from their phreatic surfaces to the vadose zone, rather than gain water from there. Therefore, ε is positive i.e. the Poisson equaiton has a sink term. Also, the roots of phreatophites transpire with the same sink-effect. Instead of mounds, groudnwater troughs are formed, especially, in catchments with intensive pumping (Kacimov et al., 2009). These troughs may become so deep that the phreatic surface reaches the bedrock, which confines the shallow aquifer from below, and unsaturated "gaps" are formed (Kacimov et al., 2004). Physically, no groundwater exists in these zones and the fronts (unknown free boundaries) emerge in Fig.1, sketched there as G_d. In a mathematical parlance, the "support" domain of the initital Poisson equation shrinks and becomes a part of solution. However, in these "gaps" an unsaturated moisture flow continues, commingled with the groundwater flow. Overall, evapotranspiration, capillarity, gravity and Darcian resistance of the porous matrix are intricately juxtaposed in problems with positive ε (or a similar S-sink term in the Richards equation). *Apriori* unknown unsaturated lacunae complicate the mathematical tasks of determination of the flow characteristics: the fields of piezometric heads, streamlines, isotachs, isobars and isohumes.

A unique hydrological situation has emerged in rapidly growing cities of the Gulf countries, in

particular, in Muscat: the virgin water table prior to urban development was so deep (often 10 + m under the ground surface) that even in hot and dry climatic conditions evaporation from it could be safely ignored. However, a recent ground surface pavement (construction of roads, buildings, car parks, etc.) in large urban areas, as well as extermination of the wild vegetation, reduced evapotranspiration and the water table rose dramatically, causing a pernicious waterlogging of the urban infrastrcuture (see e.g. Al-Sefri and Şen, 2006, Al-Senafy et al, 2015, Alsharhan and Rizk, 2020, Kreibich and Thieken, 2008). Therefore, evapotranspiration has become a vital component of hydrological balances. Moreover, municipalities and communities (severley affected by groundwater inundation) started to implement phyto-engineering measures aimed at combatting the groundwater inundation by attempts to enhance evapotranspiration. In other words, urban plants are cultivated not only for ornamental (beautification) purposes but as bioengineers, the main purpose of which is desaturation by intensive transpiration of a critical zone in the urban subsurface (Fig.2a). In the Gulf, the situation is exacerbated by the lack of evapotranspiration-related hypdropedological and hydrogeological data on the subsurface. Indeed, a common perception of urban planners in the Gulf was always a “deep water table”, with no threats of waterlogging. Unlike humid and semi-humid regions of Europe (e.g. UK, Germany, Switzerland), where the urban groundwater is monitored for centuries and the trend of its recent rise is well undesrstood (see e.g. Minnig et al., 2018, Moeck et al., 2018), in Oman the corrresponding studies have just started (Kacimov et al., 2020b). The local hydrologists, engineers and mathematicians are urged to conceive at least estimates of the ongoing groundwater inundation and to offer adequate models of groundwater and vadose zone flows, as a component for urban planning.

This paper is organized as following. In Section 2-3, we estimate the volume of groundwater and area of an unsaturated “gap” by the help of a model based on the Dirichlet’s BVP to the Poisson equation with a constant RHS (evaporation intensity). In Section 4, the PDE becomes nonlinear

because evapotranspiration exponentially decreases with the depth of the water table. In Section 5, we use HYDRUS and solve a mixed BVP to the Richards equation, which models evaporation from the water table subtending or "fingering" into a vadose zone. In Appendix 1 (Electronic Supplementary File 2), we provide some details on the confomal radius of planar domains.

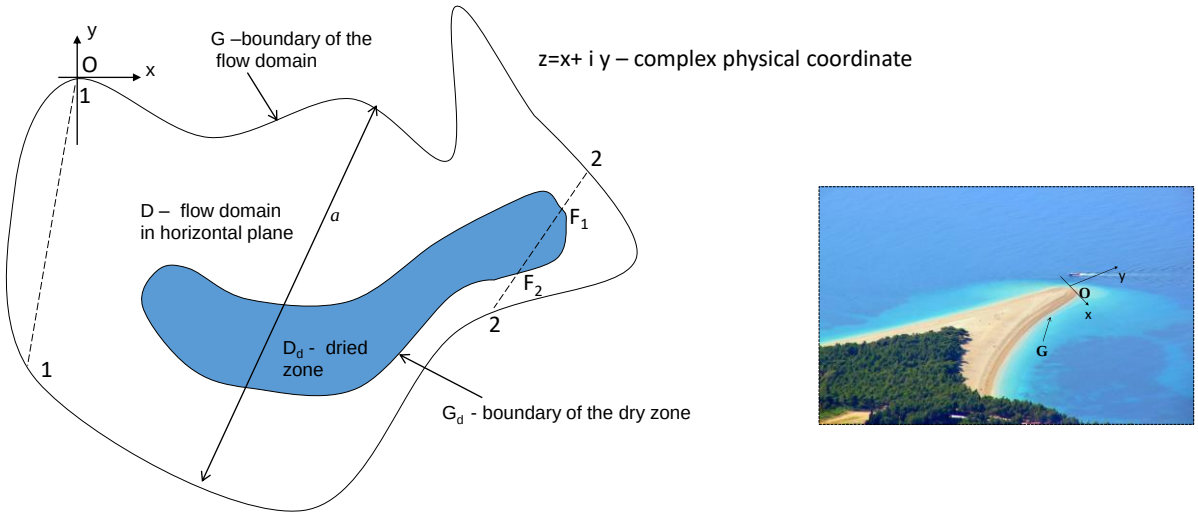

Fig. 1. Plan (aerial) view of an unconfined aquifer.

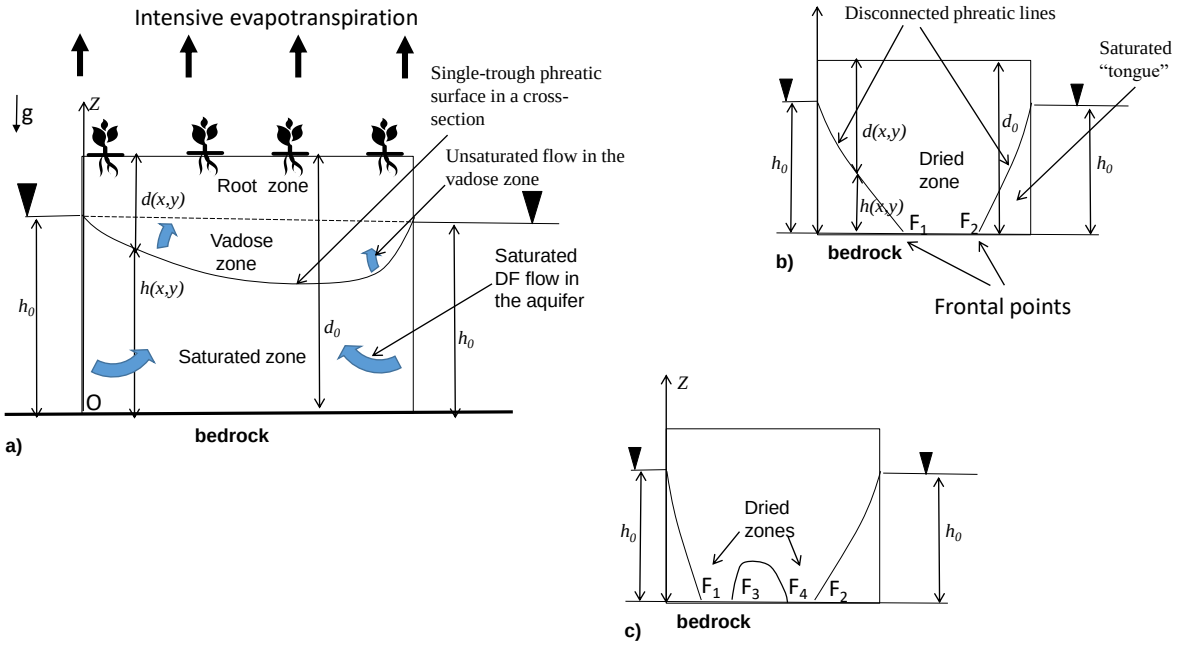

Fig.2. Vertical cross-sections. Unconfined aquifer with: no unsaturated lacunae a), one lacuna b), two lacunae c).

2. Constant Evaporation Rate

We assume that without evaporation (e.g. during the winter season in Muscat) and/or prior to phyto-drainage (no transpiration), groundwater in an unconfined homogeneous and isotropic aquifer is static i.e. we neglect a regional flow. Therefore, the water table is horizontal, at an elevation h_0 (m) above a horizontal impermeable bedrcok (Fig.1-2). A flat soil surface is at the level d_0 (m) above the bedrock. D has a characteristic size a (m).

The land surface in zone D may be covered by xerophitic plants (e.g. *Australian prosopis* reeds, Ghaf tree, Christ's thorn tree, acacia tortilis, eucaleptus, or other species), which intensively uptake soil water from the vadose zone (and, perhaps, even from the saturated zone) such that evapotranspiration from D is even higher than from a bare soil. Examples of phreatophitic plants

growing over a shallow water table in Oman are illustrated in the Photogallery (Electronic Supplementary File 1) attached to this MS; an example of a designed wetland is presented in Zhang et al. (2020).

The domain D (for simplicity assumed to be simply-connected in Fig.1) is bounded by a closed curve *G* (e.g. a drainage ditch). Kacimov et al. (2016), Toller and Strack (2019) modeled D as a promontory (see photo in Fig.1) or island.

Evapotranspiration induces pore water flow from *G* into D in the following way: the saturated flow is quasi-horizontal and the vadose zone flux (controlled by root water uptake and evaporation) is quasi-vertical. In the analytical (steady) solutions (Sections 2-3), capilarity is ignored. In Section 4, a transient saturated-unsaturated 3-D flow is numerically studied.

If evapotranspiration is very high (or h_0 is small, or a is large), then a subdomain $D_d \subset D$ can form (Kacimov et al., 2004). There is no saturated groundwater inside D_d. Fig.2a shows a vertical cross-section 1-1 (Fig.1) without an unsaturated lacuna, whereas Fig.2b depicts another cross-section 2-2 (see also Fig.1) in which two saturated tongues extend into D up to frontal points F_1 and F_2 i.e. the phreatic line in Fig.2b tapers towards these points from the left and right (zone D in Fig.1 is double-connected)

Obviously, even in a double-connected D and simply-connected D_d (Figs. 1 and 2b) we can get two or more disconnected unsaturated zones D_{d1}, D_{d2},… In other words, depending on the choice of the cross-section 2-2 (Fig.1), more than two frontal points can exist (see e.g. a vertical section in Fig.2c where two unsaturated lacunae and four frontal points are shown).

In this Section, we select cartesian coordinates *xyZ*O (Figs.1 and 2); the vertical axis O*Z* is counteroriented with the gravitaitonal acceleration.

In D, we follow Strack (2017,a, Chapter 2) and consider a vertically-averaged flow in the x, y-directions of Fig.1. In other words, we employ the Dupuit-Forchheimer (hereafter abbreviated as DF) approximation (valid for domains D with sufficiently small h_0/a in Fig.2a). Strictly speaking, flow regimes in Fig.2b,c require a full 3-D groundwater flow analysis, which even in 2-D flows with non-vertical trench boundaries AC is cumbersome (Kacimov et al., 2004, 2016).

In the DF model, the saturated thickness of the aquifer is $h(x,y)$ (m). Aquifer's conductivity is K (m/day) and we first assume the evaporation rate ε (m/day) to be independent of the depth of the water table such that $e = const = 2\varepsilon/K > 0$. It is well-known (Polubarinova-Kochina, 1962, Strack, 2017 a) that $h(x,y)$ obeys the linear Poisson PDE:

$$\frac{\partial^2 h^2(x,y))}{\partial x^2} + \frac{\partial^2 h^2(x,y))}{\partial y^2} = e, \quad e > 0 \qquad (1)$$

In what follows, we impose the Dirichlet boundary condition along G :

$$h_g = h_0, \quad h_0 = const > 0, \quad h_0 \le d_0 \qquad (2)$$

Eqn. (2) is an approximation of variable (in space) boudnary conditions in drainage ditches, rivers and their tributaries, wadis, etc. Mixed BVPs to eqn.(1) modeling seepage have been solved in Kacimov et al. (2020a).

Physically, h>0 for groundwater and h=0 corresponds to G_d in Figs.1, 2b,c. One of the key integral charactersitics of a hydrological system is the total groundwater storage in D:

$$V_w = \iint_D h(x,y)dxdy. \qquad (3)$$

Explicit calcualtion of V_w is possible for simple shapes of D only, when the BVP can be analytically solved. For arbitrary D, reasonable bounds of V_w are needed such that solution to the BVP is circumvented. Thus, we formulate:

Problem 1. Estimate V_w.

We suppose that there exists $h(x,y) \geq 0$ on the domain D. For positive e, $h(x,y) < h_0$. Consequently,

$$V_w = \iint_{\mathrm{D}} h(x,y)dxdy < h_0 A(\mathrm{D}),$$

where $A(\mathrm{D})$ is the area of the domain D. Clearly, there exists a quantity $\kappa = \kappa(e, h_0, \mathrm{D})$ such that

$$0 < \kappa(e, h_0, \mathrm{D}) < h_0 A(\mathrm{D}) \qquad (4)$$

and

$$V_w = \iint_{D} h(x,y)dxdy = h_0 A(\mathrm{D}) - \kappa(e, h_0, \mathrm{D}), \quad (5)$$

Obviously, the inequalities (4) are trivial.

Our main aim is to obtain non-trivial bilateral estimates of $\kappa = \kappa(e, h_0, \mathrm{D})$, better than inequalities (4). To do this we consider the domain D as a Lobachevsky plane endowed with the hyperbolic Poincaré metric[1]. More precisely, we engage the conformal radius $R(z, \mathrm{D})$ ($z = x + iy \in \mathrm{D}$) defined by the equation

$$R(z, \mathrm{D}) = \frac{1}{\lambda_D(z)}, \quad z = x + iy \in \mathrm{D},$$

where we introduced a complex variable *z;* $\lambda_D(z)$ is the coefficient of the Poincaré metric on the domain D with the Gaussian constant curvature $c = -4$.

[1] In the Appendix, we elaborate on the Poincaré metric.

In our improved estimates, we will also use a novel characersitic, $I_c(\mathrm{D})$, the conformal inertia moment of the domain D defined by Avkhadiev (1998) as follows:

$$I_c(\mathrm{D}) = \iint_D R^2(x+iy)dxdy.$$

$I_c(\mathrm{D})$ generalizes the well known moment of intertia, which in classical mechanics is evaluated with respect to a certain line, rather than a bounding curve.

Here we list several basic properties of the conformal radius (the details see in Bandle and Flucher, 1996, Avkhadiev and Wirths, 2009,):

(i) The radius $R(z,\mathrm{D})$ satisfies the non-linear Liouville equation

$$\Delta U = \exp(-2U), \quad U = U(x,y) = \ln R(z,\mathrm{D}), \quad z = x+iy \in \mathrm{D},$$

which is equivalent to the following non-linear PDE

$$R(z,\mathrm{D})\Delta R(z,\mathrm{D}) = |\nabla R(z,\mathrm{D})|^2 - 4, \quad z = x+iy \in \mathrm{D}.$$

(ii) Inside the domain D, $R(z,\mathrm{D}) > 0$ and $R(z,\mathrm{D}) = 0$ for boundary points $z \in G$.

Moreover,

$$R(f(\zeta),\mathrm{D}) \equiv |f'(\zeta)|(1-|\zeta|^2), \quad z = f(\zeta) \in \mathrm{D},$$

where f is a univalent conformal mapping of the unit disc $|\zeta| < 1$ in a reference plane $\zeta=\xi+i\,\eta$ onto the domain D.

(iii) As consequences of the Koebe one-quarter theorem and the Schwarz-Pick inequality (Garnett and Marshall, 2005 , Avkhadiev and Wirth, 2009) we have

$$\frac{1}{4}R(z,\mathrm{D}) \le dist(z,\mathrm{G}) \le R(z,\mathrm{D}), \quad z \in \mathrm{D}, \qquad (\mathrm{A1})$$

where $dist(z,\mathrm{G})$ is the distance from $z \in \mathrm{D}$ to the boundary of D, i. e.

$$dist(z,\mathrm{G}) = \min_{w\in\mathrm{G}}|z-w|, \quad z \in \mathrm{D}.$$

Clearly, the quantity $dist(z,\mathrm{G})$ is the distance between a point inside the domain and the boundary of D. Distance is common in the Euclidean geometry, i.e. is defined independent of any conformal mappings.

Now, we consider the estimates of V_w from (3) in the case, when $h(x,y)$ is solution to the BVP (1)—(2).

We prove the inequalities (6) and (7):

$$V_w = \iint_{\mathrm{D}} h(x,y)dxdy \geq h_0 A(\mathrm{D}) - \frac{e}{8\pi h_0} A^2(\mathrm{D}), \qquad (6)$$

and

$$\frac{3e}{4h_0} \leq \frac{\kappa(e,h_0,\mathrm{D})}{I_c(\mathrm{D})} \leq \frac{2e}{h_0}, \qquad (7)$$

These inequalities are equivalent to the bilateral estimates:

$$h_0 A(D) - \frac{e}{h_0}\iint_D R^2(z)dxdy \leq V_w \leq h_0 A(\mathrm{D}) - \frac{3e}{8h_0}\iint_{\mathrm{D}} R^2(z)dxdy, \qquad (8)$$

For a fixed h_0, from inequalities (8) it follows that

$$\lim_{e\to 0} V_w = h_0 A(\mathrm{D}).$$

i.e. a trivial limit of a static water table with no evapotranspiration. It is noteworthy that the rough estimate $V_w = \iint_{\mathrm{D}} h(x,y)dxdy < h_0 A(\mathrm{D})$ becomes asymptotically sharp, if the number e/h_0 is sufficiently small.

To prove the inequalities (6)—(8) we use the results from the theory of elasticity, *viz.*

torsion of bars (see e.g. Arutyunyan and Abramyan, 1963). In this theory, a characteristic function obeys the same BVP (1)-(2) but with a negative constant in the RHS of eqn.(1). In dimensionless quantities, the torsional rigidity, $P(\mathrm{D})$, of an elastic bar having a cross section D is defined (see e.g. Saint Venant, 1856, Timoshenko, 1954) by the integral

$$P(\mathrm{D}) = 2\iint_{\mathrm{D}} u(x,y)dxdy,$$

where the stress function $u = u(x,y)$ is the solution of the Dirichlet BVP: $\Delta u = -2$ on D and $u = 0$ on G. The functional *P* quantifies the resistance to twisting of a cylindrical bar having a cross section D in Fig.1. Let now

$$u(x,y) = (2/e)(h_0^2 - h^2(x,y))$$

that gives

$$P(\mathrm{D}) = \frac{4}{e}\iint_{\mathrm{D}} (h_0^2 - h^2(x,y))dxdy,$$

where the function $h^2(x,y)$ is defined as the solution of the BVP (1)—(2). Using the simple inequalities

$$\frac{h_0^2 - h^2(x,y)}{2h_0} \le h_0 - h(x,y) \le \frac{h_0^2 - h^2(x,y)}{h_0}$$

we obtain that

$$\frac{e}{8h_0} \le \frac{\kappa(e,h_0,\mathrm{D})}{P(\mathrm{D})} \le \frac{e}{4h_0}, \qquad (9)$$

and that

$$h_0 A(\mathrm{D}) - \frac{e}{4h_0}P(\mathrm{D}) \le V_w \le h_0 A(\mathrm{D}) - \frac{e}{8h_0}P(\mathrm{D}). \qquad (10)$$

According to the Saint Venant - Pòlya isoperimetric inequality (see Pòlya and Szegö, 1951, Timoshenko, 1954):

$$P(\mathrm{D}) \le \frac{A^2(\mathrm{D})}{2\pi}.$$

Applying this inequality and the left hand site inequality in (10), we get the inequality (6).

We obtain the estimates (7) and (8) by using (9) and (10) and applying the bilateral estimates

$$I_c(\mathrm{D}) \le P(\mathrm{D}) \le 4I_c(\mathrm{D})$$

obtained by Avkhadiev (1998), as well as the isoperimetric inequality $(3/2)I_c(\mathrm{D}) \le P(\mathrm{D})$ of Salahudinov (2001).

Remark. The quantity *P(*D) has been evaluated and utlized in mechanics of soilid bodies and fluids, see, e.g. Saint Venant (1856), Pòlya and Szegö (1951), Timoshenko (1954), Arutyunyan and Abramyan, 1963, Bandle (1980), Avkhadiev and Kacimov (2002), Carbery et al. (2014), Kacimov et al. (2017a), Avkhadiev (1995, 2015, 2020), Keady and Wiwatanapataphee (2020). One can readily obtain several estimates, similar to (6)–(8), using other known results on the quantity $P(D)$ and eqn. (10). In particular, one can apply the classical formulas by Cauchy and Saint Venant (see Timoshenko, 1954, Arutyunyan and Abramyan, 1963):

$$P(\mathrm{D}) \approx 4\frac{I_x I_y}{I_p}, \quad P(\mathrm{D}) \approx \frac{A^4}{4\pi^2 I_p}.$$

Here I_p, I_x, I_y are the inertia moments of D:

$$I_p = \iint_D [(x-x_0)^2 + (y-y_0)^2]dxdy,$$

$$I_x = \iint_D (y-y_0)^2 dxdy, \quad I_y = \iint_{\mathrm{D}} (x-x_0)^2 dxdy,$$

where the point (x_0, y_0) is the center of mass of D.

3. Lower and upper estimates for the area of the unsaturated zone

As we have mentioned, in hydroecological applications it is important to know the size of $\mathrm{D_d}$, in particular its area $\mathrm{A_d}$ (shaded in Fig.1a). Specifically, the roots of phreatophytes, if located in $\mathrm{D_d}$, can not get water from the water table i.e. the plants there may wilt.

Similarly to Problem 1, we formualte

Probem 2. Estimate A_d.

In order to solve this Problem we inscribe circles into D. Let $\delta_0 > 0$ be the Euclidean inradius defined by

$$\delta_0 = \max_{z \in \mathrm{D}} dist(z, \mathrm{G}).$$

It is evident that δ_0 as a minimax is the radius of the largest circle, inscribed in the domain D and there exists a disc $\mathrm{D}(x_0, y_0, \delta_0)$ such that

$$\mathrm{D}(x_0, y_0, \delta_0) = \{(x, y): (x - x_0)^2 + (y - y_0)^2 < \delta_0^2\} \subset \mathrm{D}.$$

Again, we draw an analogy with the theory of elasitcity and consider the Saint Venant stress function, $u = u(x, y)$, defined as the solution of the BVP: $\Delta u = -2$ on D and $u = 0$ on G.

In view of the identity $u(x, y) = (2/e)(h_0^2 - h^2(x, y))$, the domain $\mathrm{D_d}$ is defined by

$$\mathrm{D_d} = \{(x, y) \in \mathrm{D}: u(x, y) > (2/e)h_0^2\}.$$

Assume that

$$\delta_0 > \frac{2\ h_0}{\sqrt{e}}. \qquad (11)$$

If the condition (11) on the Euclidean inradius δ_0 is valid for D, then the unsaturated domain D_d is not an empty set.

Indeed, from comparing *u(x,y)* with the stress function for the inscribed disc $\mathrm{D}(x_0, y_0, \delta_0)$ the inequality follows:

$$u(x,y) \geq \frac{1}{2}\left(\delta_0^2 - (x-x_0)^2 - (y-y_0)^2\right), \qquad (x,y) \in \mathrm{D}(x_0, y_0, \delta_0) \quad \text{(A2)}$$

Consequently,

$$\left\{ (x,y) \in \mathrm{D} : \delta_0^2 - (x-x_0)^2 - (y-y_0)^2 > \frac{4h_0^2}{e} \right\} \subset \mathrm{D_d}$$

Therefore, the domain $\mathrm{D_d}$ contains the disc $\left\{ (x,y) \in \mathrm{D} : (x-x_0)^2 + (y-y_0)^2 < \delta_0^2 - \frac{4h_0^2}{e} \right\}$. Thus if the inequality (11) is valid, then

$$A_d \geq \pi\left(\delta_0^2 - \frac{4h_0^2}{e}\right)$$

Evidently, if D is a disc, then this inequality is sharp.

Next, suppose that there exists a domain $\mathrm{D_d}$ and we target an upper estimate of its area A_d.

Since the stress function $u(x,y) \geq 0$ on D and $u(x,y) \geq (2/e)h_0^2$ on $\mathrm{D_d}$, one immediately obtains

$$P(\mathrm{D}) = 2\iint_{\mathrm{D}} u(x,y)dxdy \geq 2\iint_{\mathrm{D_d}} u(x,y)dxdy \geq (4/e)h_0^2 A_d.$$

that yields

$$A_d \leq \frac{e}{4\,h_0^2}\, P(\mathrm{D}).$$

Now, one can apply the known isoperimetric inequalities for the torsional rigidity. In particular, one has the following inequalities:

$$A_d \leq \frac{e}{8\pi\, h_0^2}\, A^2(\mathrm{D}), \quad A_d \leq \frac{e}{h_0^2}\,\frac{I_x I_y}{I_p}, \quad A_d \leq \frac{eI_c}{h_0^2}$$

Example 1. Consider a disc as domain D. Namely, we take

$$\mathrm{D} = \mathrm{D}(x_0, y_0, r_0) = \{(x,y): (x-x_0)^2 + (y-y_0)^2 < r_0^2\}, \quad r_0 > 0.$$

The solution of the BVP (1)—(2) for infiltration (negative RHS in eqn.(1)) is (Strack, 2017a)

$$h^2(x,y) = \frac{e}{4}[(x-x_0)^2 + (y-y_0)^2] + h_0^2 - \frac{e}{4}r_0^2.$$

Assume that

$$h_0 \geq \frac{\sqrt{e}}{2} r_0,$$

then $h(x,y) \geq 0$ at every point of the disc i.e. no dried zone emerges at the centre. For this case, straightforward computations and some algebra give that

$$V_w = \iint_{\mathrm{D}} h(x,y)dxdy = \frac{8\pi}{3e}\left(h_0^3 - \left(\sqrt{h_0^2 - er_0^2/4}\right)^3\right) =$$

$$= \frac{2A}{3} h_0 \left(\tau + \frac{1}{1+\tau}\right), \qquad \text{(A3)}$$

where $\tau = \sqrt{1 - er_0^2/(4h_0^2)} \in [0,1)$ and $A = \pi r_0^2$ is the area of the disc. It is evident that

$$\frac{2}{3} \leq \frac{V_w}{Ah_0} < 1. \qquad \text{(A4)}$$

Next, assume that

$$0 < h_0 < \frac{\sqrt{e}}{2} r_0.$$

Evidently, in this case $\mathrm{D_d}$ is a smaller “internal” disc

$$(x-x_0)^2 + (y-y_0)^2 < r_d^2, \quad r_d = \sqrt{r_0^2 - \frac{4}{e}h_0^2},$$

and

$$A_d = \pi\left(r_0^2 - \frac{4}{e}h_0^2\right), \quad V_w = \int_{\mathrm{D}\setminus\mathrm{D_d}} h(x,y)dxdy = \frac{8\pi}{3e}h_0^3 \quad \text{(A5)}$$

Example 2. Let D is an ellipse with semiaxes a_0 and b_0. Namely, we assume that

$$\mathrm{D} = \mathrm{D}(x_0, y_0, a_0, b_0) = \left\{(x,y): \frac{(x-x_0)^2}{a_0^2} + \frac{(y-y_0)^2}{b_0^2} < 1\right\}, a_0 > 0, b_0 > 0.$$

Similarly to Strack (2017a, Section 2.5.8), who tackled the Poisson equation with a negative RHS, the BVP (1)—(2) has the solution defined by

$$h^2(x,y) = \frac{e\, a_0^2\, b_0^2}{2(a_0^2+b_0^2)}\left(\frac{(x-x_0)^2}{a_0^2} + \frac{(y-y_0)^2}{b_0^2}\right) + h_0^2 - \frac{e\, a_0^2\, b_0^2}{2(a_0^2+b_0^2)}.$$

The condition $h(x,y) \geq 0$ on $\mathrm{D}(x_0, y_0, a_0, b_0)$ is equivalent to the inequality

$$h_0 \geq \frac{a_0\, b_0\sqrt{e}}{\sqrt{2(a_0^2+b_0^2)}}.$$

Using the generalized polar coordinates $x = a_0 r\cos\theta$, $y = b_0 r\sin\theta$ by straightforward computations we obtain

$$V_w = \iint_{\mathrm{D}} h(x,y)dxdy = \frac{4\pi(a_0^2+b_0^2)}{3ea_0b_0}\left(h_0^3 - \left(\sqrt{h_0^2 - \frac{e\, a_0^2\, b_0^2}{2(a_0^2+b_0^2)}}\right)^3\right] =$$

$$= \frac{2A(a_0,b_0)}{3} h_0 \left(\tau_0 + \frac{1}{1+\tau_0}\right),$$

where $\tau_0 = \sqrt{1 - e(a_0^2+b_0^2)/(2a_0^2b_0^2h_0^2)} \in [0,1)$ and $A(a_0,b_0) = \pi a_0 b_0$ is the area of the domain $\mathrm{D}(x_0, y_0, a_0, b_0)$. Again, we obtain that

$$\frac{2}{3} \leq \frac{V_w}{A(a_0,b_0)h_0} < 1.$$

Now, we assume that

$$0 < h_0 < \frac{a_0\, b_0\sqrt{e}}{\sqrt{2(a_0^2+b_0^2)}}.$$

For this case, the domain $\mathrm{D_d}$ is

$$\frac{e\, a_0^2\, b_0^2}{2(a_0^2+b_0^2)}\left(\frac{(x-x_0)^2}{a_0^2} + \frac{(y-y_0)^2}{b_0^2}\right) < \frac{e\, a_0^2\, b_0^2}{2(a_0^2+b_0^2)} - h_0^2$$

and G_d is a small "internal" ellipse, the area of which is

$$A_d = \pi a_0 b_0 \left(1 - \frac{2\,h_0^2\,(a_0^2+b_0^2)}{e\,a_0^2\,b_0^2}\right).$$

4. The Evaporation Rate Varying with Depth

In this Section, we consider the evaporation rate decreasing with the depth of the water table, $d(x,y) = d_0 - h(x,y)$ (Fig. 2). Linear or nonlinear functions $e(d)$ were experimentally examind (see, e.g., Hu et al., 2008, Katz, 1968, PK-62, Shokri-Kuehni et al., 2019).

Without any loss of generality, we select the exponential function in the RHS of the Poisson equation (Kacimov et al., 2019). Then the BVP (1)-(2) is transformed into a nonlinear one:

$$\frac{\partial^2 h^2(x,y))}{\partial x^2} + \frac{\partial^2 h^2(x,y))}{\partial y^2} = e_0 exp[-\lambda d(x,y)], \quad (12)$$

where

$$e_0 = const > 0, \;\; \lambda = const \geq 0, d_0 = const \geq h_0 = const \geq 0, h_G = h_0.$$

Probem 3. Estimate V_w and A_d.

Again, we engage the classical Saint Venant model. Namely, we use the earleir defined torsional rigidity $P(D)$ where the function $u = u(x,y)$ is superharmonic one, defined as the solution of the BVP: $\Delta u = -2$ on D and $u = 0$ on G.

Assume that there exists the solution $h(x,y)$ such that $0 \leq h(x,y) \leq h_0$ at every point $(x,y) \in D$. We use eqn. (12) and the estimates

$$e_0 exp[-\lambda d_0] \leq \Delta h^2(x,y) = \frac{\partial^2 h^2(x,y))}{\partial x^2} + \frac{\partial^2 h^2(x,y))}{\partial y^2} \leq e_0 exp[-\lambda(d_0 - h_0)]$$

juxtaposed with the equation

$$\Delta u(x,y) = \frac{\partial^2 u(x,y)}{\partial x^2} + \frac{\partial^2 u(x,y)}{\partial y^2} = -2,$$

That yileds

$$\Delta\left(-h_0^2 + h^2(x,y) + \frac{e_0}{2} exp[-\lambda d_0]\, u(x,y)\right) \geq 0$$

and the inequality

$$\Delta\left(-h_0^2 + h^2(x,y) + \frac{e_0}{2} exp[-\lambda (d_0 - h_0)]\, u(x,y)\right) \leq 0$$

which holds at every point $(x,y) \in D$. Since the functions $-h_0^2 + h^2(x,y)$ and $u(x,y)$ vanish on the boundary of the domain, we get

$$\frac{e_0}{2} exp[-\lambda d_0] u(x,y) \leq h_0^2 - h^2(x,y) \leq \frac{e_0}{2} exp[-\lambda (d_0 - h_0)] u(x,y) \qquad (13)$$

at every point $(x,y) \in \mathrm{D}$. By integrating we obtain

$$\frac{e_0}{4} exp[-\lambda d_0] \leq \frac{\iint_D \left(h_0^2 - h^2(x,y)\right) dxdy}{P(D)} \leq \frac{e_0}{4} exp[-\lambda (d_0 - h_0)]. \qquad (14)$$

Using inequalities (14) and the inequalities

$$(h_0^2 - h^2(x,y))/(2h_0) \leq h_0 - h(x,y) \leq (h_0^2 - h^2(x,y))/h_0,$$

we get

$$\frac{e_0}{8h_0} exp[-\lambda d_0] P(\mathrm{D}) \leq h_0 A(\mathrm{D}) - V_w \leq \frac{e_0}{4h_0} exp[-\lambda (d_0 - h_0) P(\mathrm{D}). \qquad (15)$$

From inequalities (15) it follows that

$$V_w \approx h_0 A(\mathrm{D}),$$

if the quantity e_0 is sufficiently small.

Using inequalities (15) and the known inequalities for the torsional rigidity $P(\mathrm{D})$ one can find several estimates for V_w. We present here two of them. Applying (15) and the Saint Venant-Pòlya isoperimetric inequality $P(\mathrm{D}) \leq A^2(\mathrm{D})/(2\pi)$, we obtain that

$$V_w \geq h_0 A(\mathrm{D}) - \frac{e_0}{8\pi h_0} exp[-\lambda (d_0 - h_0)] A^2(\mathrm{D}).$$

Applying the bilateral estimates $(3/2)I_c(\mathrm{D}) \le P(\mathrm{D}) \le 4I_c(\mathrm{D})$ that are valid for every simply connected domain D, one gets

$$\frac{3e_0}{16h_0} exp[-\lambda d_0] \le \frac{h_0 A(D) - V_w}{\iint_{\mathrm{D}} R^2(x+iy,D)dxdy} \le \frac{e_0}{h_0} exp[-\lambda(d_0 - h_0). \quad (16)$$

By the above-used property (A1) of the conformal radius we obtain

$$\iint_{\mathrm{D}} dist^2(z,\mathrm{G})dxdy \le \iint_{\mathrm{D}} R^2(z,\mathrm{D})dxdy \le 16 \iint_D dist^2(z,\mathrm{G})dxdy. \quad (17)$$

Inequalities (16) and (17) imply the following estimates

$$\frac{3e_0}{16h_0} exp[-\lambda d_0] \le \frac{h_0 A(D) - V_w}{\iint_{\mathrm{D}} dist^2(x+iy,G)dxdy} \le \frac{16e_0}{h_0} exp[-\lambda(d_0 - h_0),$$

Lower and upper estimates for the area of the unsturated zone

First, we assume that

$$\delta_0 > \frac{2h_0}{\sqrt{e_0}} \exp(\lambda d_0 / 2) \quad (18)$$

where δ_0 is the Euclidean inradius of the domain D. Using the estimate (A2) and the left hand side in eqn.(13) we infer the following: if the inequality (18) is satisfied, then $\mathrm{D_d}$ is not an empty set and

$$A_d \ge \pi\left(\delta_0^2 - \frac{4h_0^2}{e_0} \exp(\lambda d_0 / 2)\right)$$

Now, suppose that the domain D_d is not an empty set. We obtain an upper estimate of the area A_d of D_d.

The stress function $u(x,y) \ge 0$ on D. From the RHS of inequality (13) it follows that $u(x,y) \ge (2/e_0)h_0^2 \exp(\lambda(d_0 - h_0))$ at any point $(x,y) \in D_d$. From this inequality, it follows that

$$P(D) = 2\iint_D u(x,y)dxdy \ge 2\iint_{D_d} u(x,y)dxdy \ge (4/e_0)h_0^2 \exp(\lambda(d_0 - h_0))\, A_d.$$

437 Therefore,

438 $$A_d \le \frac{e_0}{4\,h_0^2}\exp(-\lambda(d_0-h_0))\,P(D).$$

439 Applying the known isoperimetric inequalities for *P*(D), one has the following inequalities:

440 $$A_d \le \frac{e_0}{8\pi\,h_0^2}\exp(-\lambda(d_0-h_0))\,A^2(D), \quad A_d \le \frac{e_0}{h_0^2}\exp(-\lambda(d_0-h_0))\,\frac{I_x I_y}{I_p}. \qquad (19)$$

441

442 ## 5. HYDRUS Simulations

443 In this Section, we use HYDRUS (Šimůnek et al., 2016), which is a finite element code solving a

444 3-D transient Richards' equation:

$$\frac{\partial\theta}{\partial t} = \nabla\left(K(p)\nabla h\right) - S, \qquad (20)$$

where $\theta(t,x,y,Z)$=volumetric moisture content,

$K(p)$ = theVan Genuchten's hydrualic conductivity funnction,

445 $h(t,x,y,Z) = p + Z$ = total head, p= pressure head, Z=vertical coordinate,

S = volume of water uptake by plant roots from a volume of soil per time (1/s),

$S = S_p\alpha(h), S_p$ = potential water uptake rate (1/s),

α = Feddes' stress response function (unitless), $0 \le \alpha \le 1$

446

447 Eqn.(20) generalizes the model used in Sections 2-4 by taking into account the unsaturated zone

448 and capillarity of the soil. Even in humid countries where the phreatic surface is a netto-recipient of

449 water from the vadose zone, flow in the capillary fringe and unsaturated zone, conjugated with

450 groundwater beneath, is not so trivially-vertically 1-D (see e.g. Hunt et al., 2008, Silliman et al.,

451 2002), as often misconcepted.

452 In this Section, we use the notation *p(t,x,y,Z)=h-Z* for the pressure head[2], *x* for the radial

[2] In HYDRUS, the pressure head is denoted as h that is contrary to standard notation in groundwater hydrology where h is reserved for the total (piezometric) head (see e.g. PK-62, Strack, 2017)

453 coordinate (we solve axisymmetric problems), and ∇ is the corresponding nabla operator.

454 For comparisons with analytical results, we engage the following options of HYDRUS-3D:

455 • "2D –Axisymmetric Vertical Flow" for a circular G in Sections 2-4

456 • transient seepage during the time interval $0 < t < T$; at t=0 a certain initial
457 condition in a 3-D porous domain is selected for $p(0,x,y,Z)$; T is the simulation time
458 (we fixed it to be 600 days) at which flow becomes steady-state and, therefore,
459 comparisons with the analytical solutions in Sections 2-4 are possible

460 • a default HYDRUS initial condition of p=-100 cm in the whole flow domain is used

461 • default HYDRUS iteration criteria, time step controls, and internal interpolation are used

462 • hysteresis-free loam from the HYDURS Soil Catalogue, with the pentad parameters,
463 which determine the Van Genuchten capillary pressure relation $p(\theta)$, is used

464

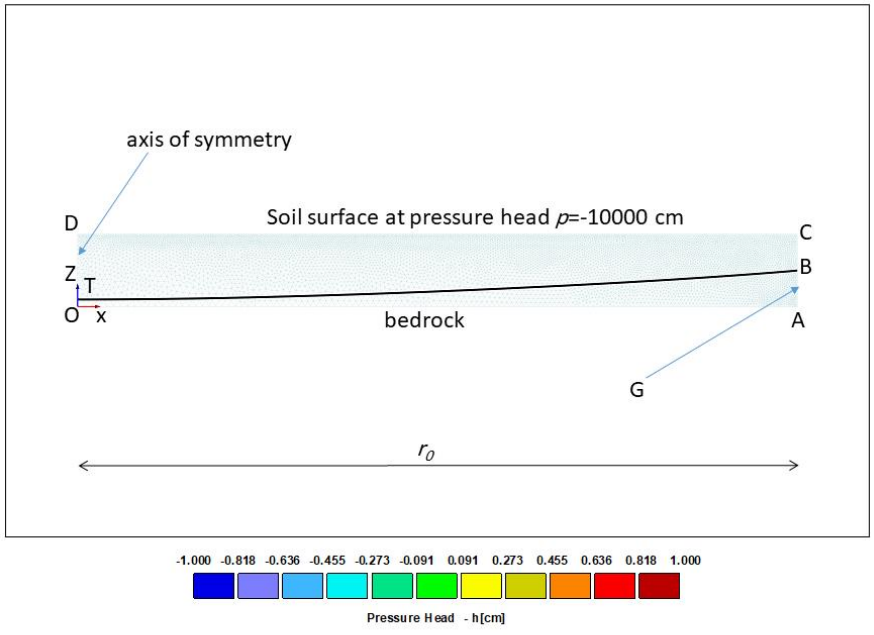

a)

465

466

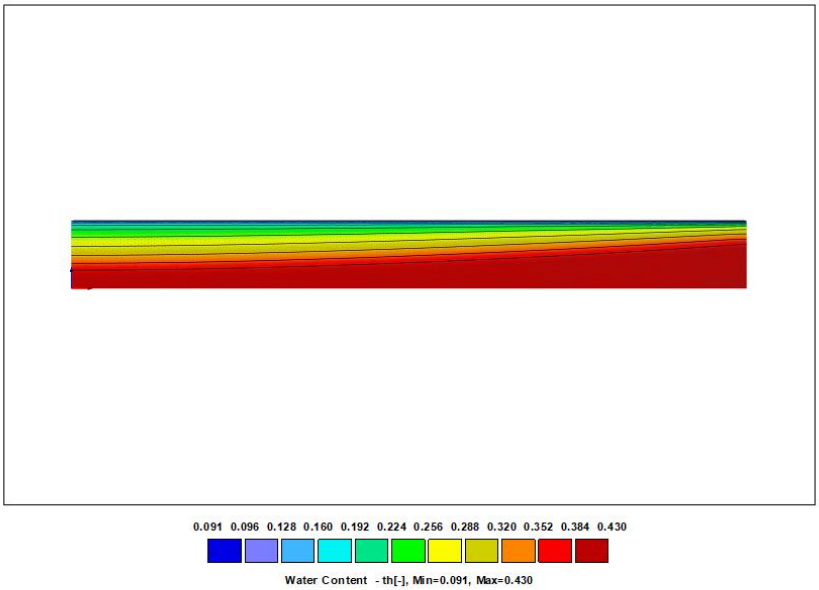

Project dryjune 8 - 50 cm -
Results, Water Content, Time 6 - 600 days

b)

467

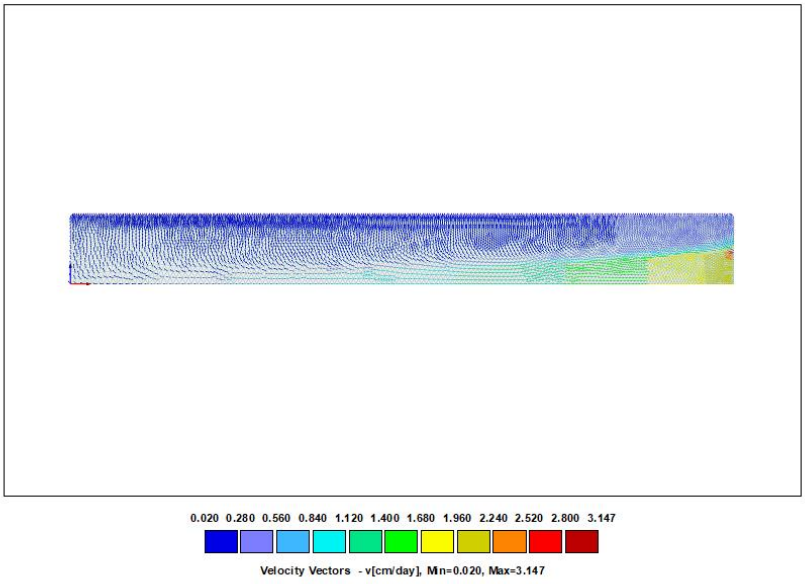

Project dryjune 8 - 50 cm -
Results, Velocity Vectors, Time 6 - 600 days

c)

468

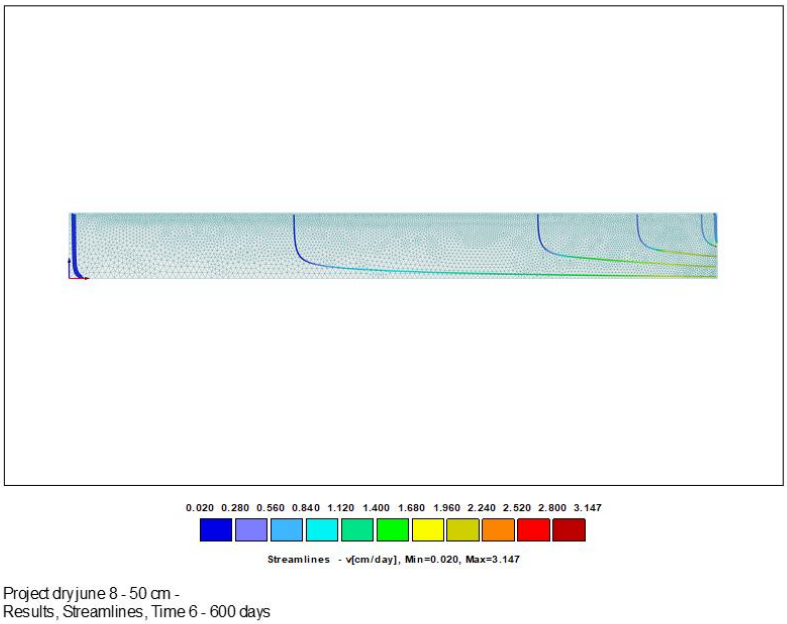

d)

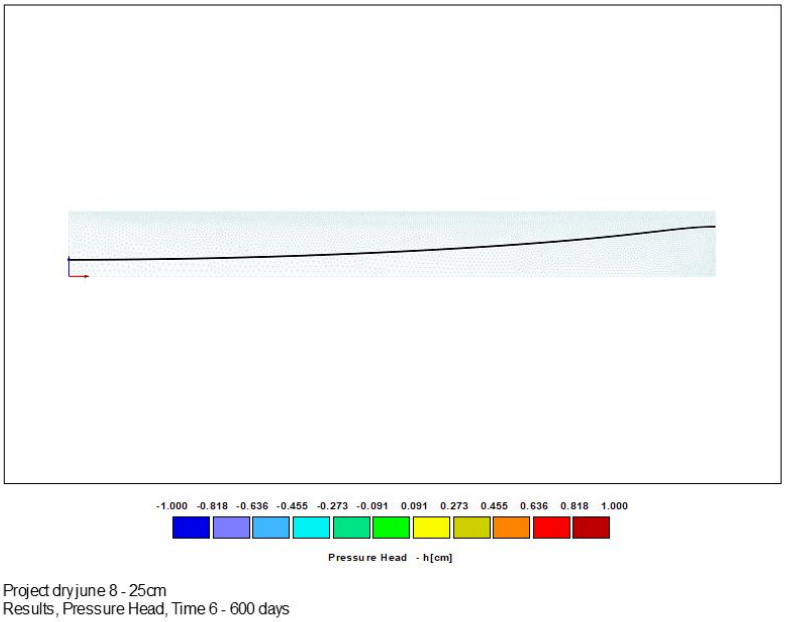

e)

Fig.3. HYDRUS simulations for saturated-unsaturated axisymmetric flow in a circular cylinder having r_0=10 m at t=600 days: a) phreatic surface TB for |AB|=50 cm.; b) isohumes $\theta(x,Z)$; c)

vectors of Darcian velocities; d) streamlines; e) phreatic surface with concave-up and concave-down segments for |AB|=75 cm.

In simulations shown in Figs.3-4 we assumed no transpiration i.e. S=0 in the RHS of eqn.(20).

Fig.3 presents the results of simulations for the case of flow without an unsaturated "gap". In this HYDRUS project, we selected a porous cylinder of a radius r_0=10 m (see Example 1 in Section 3). Due to symmetry we show only one half of an axisymmetric section. The vertical coordinate OZ coincides with the axis of symmetry, the horizontal (radial) axis Ox coincides with the bedrock. In the selected cross-section, the flow domain is a rectangle OABC. We assumed the soil thickness d_0 =1 m.

The boundary conditions are: no flow along OA (an impervious substratum), OD (the line of symmetry) and BC. The latter condition is common in the Vedernikov-Bouwer model (see e.g. PK-62, Kacimov et al., 2019) and is physically justified by the fact that evaporation from vertical slopes of excavations (see the Photogallery) are relatively minor, compared with evaporation from a horizontal soil surface). Evaporation from segment BC can be also modeled (see Kacimov, 2006). Along DC we assumed p=-10000 cm that is equivalent to very dry soil conditions. In the field, we measured the moisture content, θ, along the soil surface and found this value in May-June to be as low as 3-5% (see the Photogallery) that is even less than $\theta(-10000)$ according to the VG function for loam in HYDRUS. In sensitivity analysis, we varied p_{DC} between -10000 cm and -1000 cm and showed that the variations of the quantitative properties shown in Fig.3 (the case of the driest soil surface) are minor. We recall that according to Philip (1991), $p_{DC} = -\infty$ corresponds to the upper bound of evaporation. Along AB in Fig.3a, the total head h=h_0=50 cm i.e. p decreases linearly upward from 50 (point A) cm to 0 (point B).

496 The targeted size of finite elements was 10 cm. The mesh was refined along AC and CD. The
497 number of mesh entities is: 7332 nodes, 498 1-D elements, and 14164 2-D elements.
498 Curve BT in Fig.3a represents a phreatic surface p=0. Point T is the bottom of the water table
499 trough. Fig.3b shows the colour map of isohumes i.e. $\theta(x,Z)$. Fig.3c illustrates the vector field of
500 Darcian velocities. This field corroborates the DF analytical model used in Sections 2-4. Indeed, in the
501 saturated zone flow is prevalently horizontal and becomes almost vertical close to the soil surface
502 (albeit, close to the phreatic line the vertical and axial components of the velocity vectors are
503 comparable). The same qualitative behavior can be inferred from the streamlines plotted in Fig.3d. In
504 Fig.3e we increased h_0 from 50 to 75 cm. As result, we see not only a drawup of the phreatic line
505 (that is trivial) but also the appearance of an inflexion point. The DF approximation can not
506 predict such points and a full 2-D potential theory is needed for comparisons with HYDRUS
507 (Craster, 1994, Kacimov et al., 2018, Kacimov and Obnosov, 2006, Kacimov and Youngs, 2005).

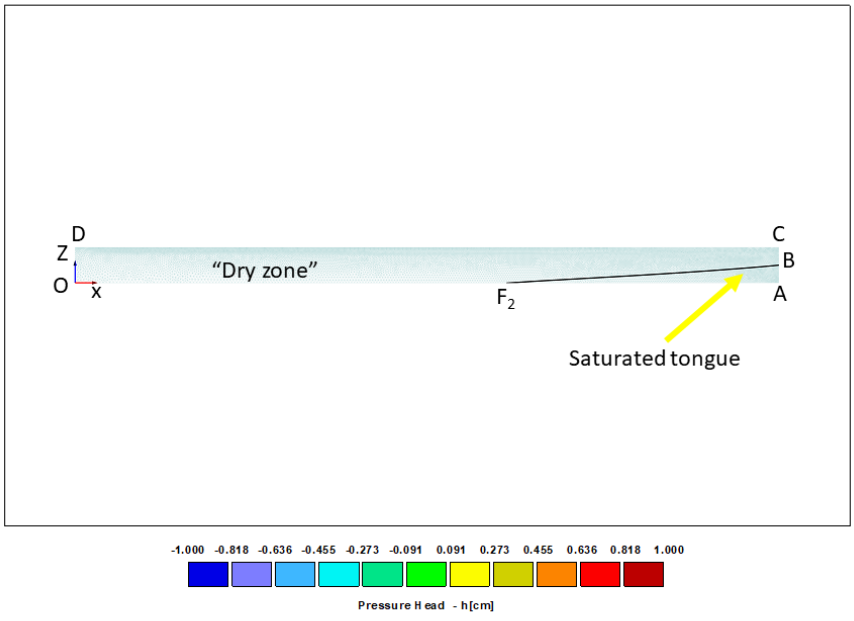

a)

508

509

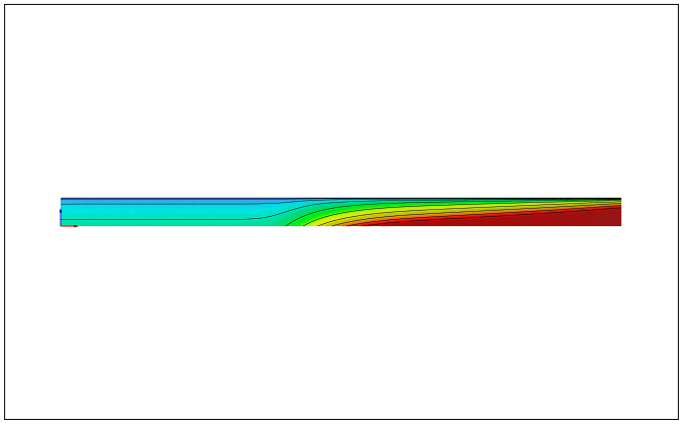

Project dry june 9 - 25cm -20m
Results, Water Content, Time 6 - 600 days

b)

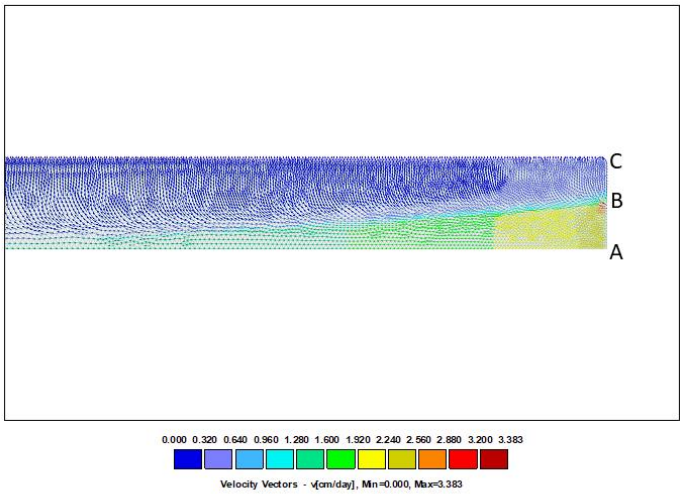

Project dry june 9 - 25cm -20m
Results, VelocityVectors, Time 6 - 600 days

c)

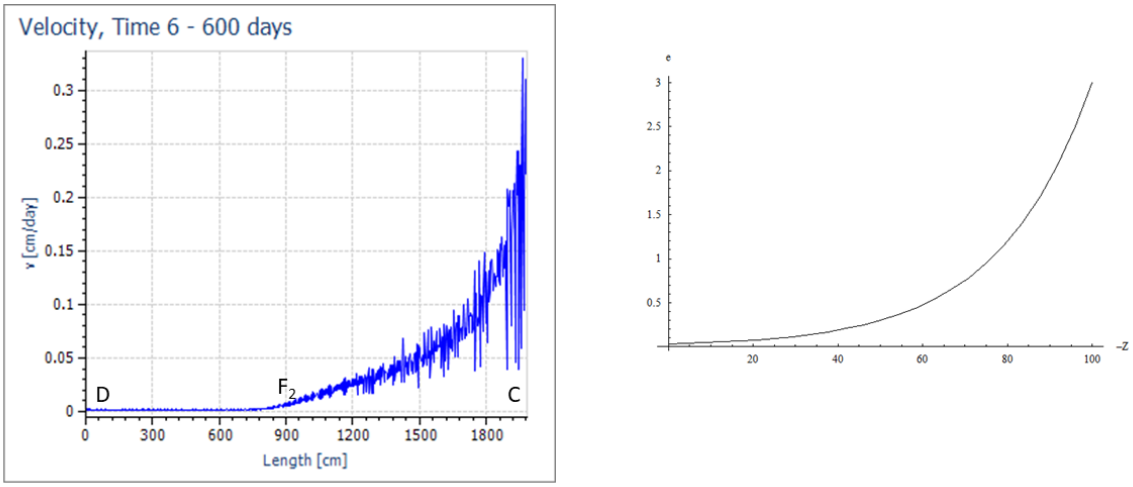

d)

512

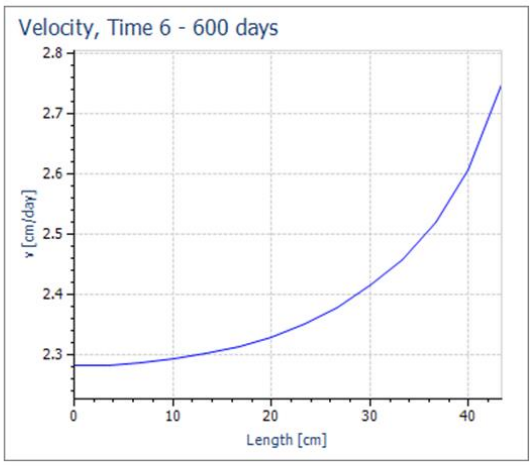

e)

513

514

515 Fig.4. HYDRUS simulations for a cylinder having r_0=20 m at t=600 days: a) phreatic surface TB

516 for |AB|=50 cm.; b) isohumes; c) Darcian velocities near AC; d) velocity magnitude along CD (left

517 panel) and evaporation rate *e(Z)* computed in Wolfram's (1991) *Mathematica* (right panel); e)
518 velocity along AB.

519

520 In Fig.4 simulation results are presented for r_0=20 m (other parameters are the same as in
521 Fig.3). In Fig.4a, a large unsaturated lacuna appears in the centre of the original 3-D porous
522 cylinder. The phreatic line BF_2 bounds a saturated "tongue" BF_2A with the coordinate of the front
523 point F_2, and r_f=12.4 m. Remarkably, BF_2, unlike a "strongly" curved BT in Fig.3a, e, is almost a
524 straight line that is in comport with the analytical solutions in terms of both the DF and potential
525 theories (Kacimov and Obnosov, 2006, 2019, Kacimov et al, 2004).

526 Fig.4b and 4c show the isohumes and velocity vectors in a zone close to G. The left panel in
527 Fig.4d presents the HYDRUS-computed magnitudes of velocity vectors along CD. The wiggling is
528 caused by numerical approximations. The right panel in Fig.4d shows "smoothening" of this curve
529 by adopting the exponentially decreasing evaporation rate, according to eqn.(12) in Section 4.
530 Specifically, we did the following: we retrieved the values of velocity at Z=1 m, $x=r_f$ and at Z=1
531 m, $x=r_0$ from HYSRUS simulations in Fig.4, *viz*. V=0.03 cm/day and 0.3 cm/day, respectively. Next,
532 we solved the system of equations

$$e_0 exp[-100 * \lambda] = 0.03,$$

$$e_0 exp[-50 * \lambda] = 0.3$$

533 with respect to e_0 and λ that gave e_0=3 cm/day and λ=0.046 1/cm. The corresponding evaporation
534 function is plotted in Fig.4d, right panel.

535 Now we compare the HYDRUS results in Fig.3-4 with the analytical solutions and estimates
536 in Sections 2-4. We selected Example 1 from Section 3.

537 First, we evaluated the HYDRUS-simulated ε from the distribution of the Darcian velocity

along CD in Fig.3a (a wiggling curve similar to one shown in Fig.4e). We used the **Interpolation** routine of *Mathematica* (interpolation order ->4) to smoothen this velocity, integrated this interpolation function from x=0 to x=1000 cm and calculated the integral average of ε=0.084 cm/day. Then, for the loam having the HYDRUS-catalogued value K=25 cm/day we got e=0.00672. Eqn. (A3) gives V_w =1.266*10^8 cm^3 and the dual bounds (A4) are: 1.047*10^8 cm^3 < V_w < 1.571*10^8 cm^3 i.e. V_w is almost perfectly an arithmetic average of the bounds. HYDRUS does not have an option to evaluate the volume of the saturated zone. So, we did the following. The water table BT in Fig.3e is a smooth curve and we selected the HYDRUS coordinates *x=0, x=100, x=200, ...,x*=1000 cm and found the corresponding Z values at which p=0. Next, we interpolated in *Mathematica* the obtained water table equation *x(Z)*. Next, we evaluated by integration of this interpolation function the volume of the body of revolution that gave us V_{wH}=9.65*10^7 cm^3 that is about 30 % less than V_w computed by the DF theory.

Second, for the case of an unsaturated "gap" (r_0=20 m) in Fig.4 we retrieved from HYDRUS the distribution of nodal values of the Darcian velocity along AB. This smooth curve is depicted in Fig.4e. We interpolated these discrete values in *Mathematica*. Next, by integrating the obtained interpolation function we evaluated an average value of velocity along AB, v_{AB}=2.39 cm/day and an approximate quantity of water seeping into the cylinder, $q_a = 2\, r_0\, h_0\, v_{AB}$= 1.5*10^6 cm^3. Next, from HYDRUS we got the radial coordinate of point F$_2$, r_{dH}=1242 cm. After that we assumed that all q_a evaporates from the phreatic surface with a constant $\varepsilon = q_a/\pi/(r_0^2 - r_{dH}^2)$ =0.194 cm/day i.e. e=0.016. Then from (A5) we evaluate A_d=1.05*10^7 cm^2 while HYDRUS gives A_{dH}= π*1242^2 =4.85*10^6 cm^2. If we assume an exponentially decreasing evaporation rate with the above-computed e_0 and λ then the first inequality in (19) gives A_d<6.13*10^6 cm^2 that well bounds A_{dH}. Overall, the discrepancy between HYDRUS and analytical results is more for the case of the unsaturated "gap" scenario as

compared with the scenario in Fig.3.

The major problem of both the DF and potential theories in modeling evaporation from a non-flat water table is in the assumption of a constant ε (see PK-77). This simplification works reasonably well if the water table is almost flat and close to the ground surface. PK and her students attempted to model ε depending on the water table depth but the obtained results in the potential (2D) model were poor.

It is noteworthy that the scenarios modeled in Figs.3-4 correspond to hyper-dry climatic conditions of the Gulf. For the climate in Holland, Rezaei et al. (2017) studied a shallow unconfined aquifer having the depth d (Fig.2) similar to ours (around 100 cm). They modeled the vadose zone flow by HYDRUS1D, assuming a quasi-flat water table, i.e. ignored both the lateral groundwater flow and 2-,3-D unsaturated flow. In the saturated-unsaturated flows pictured in Figs.3-4, evaporation is so strong that 1-D simplification in the Richards equation would be far-fetched: both lateral groundwater motion and essentially 3-D moisture flow have to be considered.

6. Concluding Remarks

Subsurface hydrologists in arid/semi-arid environemnts of the South West (Arizona, Nevada) or Australia are equipped with the opulence of multi-decadal public-domain records from a dense network of weather stations and observation piezometers, the cornucopea of various computer codes, multidiscipinary expertise of nearby academics and consultants, advanced instruments (e.g. weighing lysimeters), among others. In the deserts of Arabia, one has to muddle through limited modeling resources, in particular, scanty parametric depositaries in physcially-based models and lacunary (or even spurious) proprietary data from field observations. In this context, our paper tries to stitch the results of a simplified analytical 2D groudnwater model with ones from an advanced 3D

584 saturated-unsaturated numerical code.

585 The hydrological systems tackled in this paper are unique for the hyperarid climates of the
586 Gulf: for example in Oman, despite a very high ET_0 (3500-1500 mm/year) versus only 50-350
587 mm/year of precipitation (Empty Quarter – Jabel Al Akdar), the water table of unconfined aquifers in
588 many urban areas of Muscat (as well as in Kuwait City, Jeddah, Medina, Al-Ain, among others), has
589 risen to *d* (Fig.2) of only few cm –tens of cm from the ground surface. That has never been expected
590 and no contingecny hydrological urban planning was mulled to confront waterlogging and
591 evapotranspiration directly from the water table, which has become a crucial component of the water
592 balance of these shallow (perched) aquifers. It is noteworthy, that the focus of Western hydrologists
593 (see e.g. Hogan et al., 2004) working in arid/semi-arid regions was mostly on recharge to deep water
594 tables, i.e. evapotranspiraiton was prevalently a realm of soil physicists who work with
595 "redistribution" in the vadose zone, rather than aquifers.

596 Mathematically, the dual bounds, obtained in this paper for the groundwater storage and areal
597 extension of desaturation zone, like eqn. (A4), generalize the one-sided inequalities in the theory of
598 elasticity, electrostatics and other branches of mathematical physics, reported in the Pòlya and Szegö
599 (1951) compendium. Physically, our bounds for integral quantities of interest for arid zone
600 hydrology, serve the same purpose as pedotransfer functions. Indeed, the isoperimetric estimates of
601 Pòlya and Szegö asses an integral physical quantity, which is difficult to measure/calculate, via
602 another, which is easier to get. For example, V_w in (A3)-(A5) is not easy to find by solving the
603 Richards flow problem, while geometrical properties of D are readily determined.

604 HYDRUS3D is a wonderful package but the Richards equation requires a pentad of the Van
605 Genuchten parameters, as compared with only two in the the DF model. Also, only HYDRUS1D is a
606 free software (needs a basic training to run), while the analytical estimates, albeit based on a "crude
607 model", can be used by field hydrologists as a "back-of-an-envelope" precursor in a scaffolding

608 ascend to a more advanced and resource-consuming models. Haitjema (2006) advocated analytical
609 "equations", while our paper advocates "isoperimetric inequalities".

610 The perspectives of our work are:

611 a) In the analytical DF model, we can consider "leaky" layers, instead of an impervious
612 bedrock in Fig.2. This will transform eqn. (1) into a nonlinear modified Helmholtz
613 equation, to which we plan applying the same technique of Poincaré's metric.

614 b) Waterlogged areas in several uban districts of the Muscat governorate are currently
615 contemplated for implementing MAD (Managed Aquifer Discharge). One
616 phytoengineering option to mitigate the harm caused by a rising water table is construction
617 of reedbeds. In the numerical Richards-equation based model, we plan to involve the root
618 water uptake by desert plants (Australian *prosopis*), using the Feddes "trapezoidal" stress
619 function from HYDRUS. For this purpose, we will meter sap flow through desert
620 vegetation in Oman (HYDRUS does not have catalogued Feddes' functions for this type of
621 plants). MAD would diversify the hydrological practices-vernacular of MAR (see e.g.
622 Healy, 2010, Hogan et al., 2004).

623 c) Estimates for mixed, rather than Dirichlet's boundary conditions in the BVPs for the
624 Poisson equation (Kacimov et al., 2020a) can be attempted to derive. In HYDRUS3D a
625 new reservoir boundary condition (see e.g. Sasidharan et al., 2018), which allows
626 considering a finite water storage in the ditch (trench) depicted in Fig.2, i.e. $h_0(t)$ devoured
627 by evaporation from D via the mass-balance conservation (Al-Shukaili et al., 2020), can be
628 involved.

629 d) Even in hyper arid climates of Oman and UAE, phytoengineering (growing trees) may
630 hydrologically make the RHS of the Poisson equation negative in one part of the
631 catchment (D in Fig.1) due to enhanced infiltration during heavy surface ponding periods

(see e.g. Al-Maktoumi et al., 2020), and positive in other parts of D. Deriving isoperimetric estiamates for BVPs with an alternating sign of ε is another interesting task.

Along with the above considered dyad of integral quantities (V_w, A_d), other – local - criteria can be targeted, e.g. the ordinate of point T in case of no unsaturated lacuna (Fig.2a). If the RHS in the elliptic eqn.(1) does not change its sign inside D, the minimum principle applies for evapotranspiration regimes. Estimating the value and locus of this minimum within D, without solving the BVP itself, is improtant in ecohydrological applications.

A fascinating research area is to find optimal shapes of D, which give "sharp" Pòlya and Szegö (1951) bounds. We recall: a circular elastic bar maxes the rigidity in the class of all equi-areal bars. Does a circular D in Fig.1 possess the property of maximum V_w in case of an unsaturated lacuna? Does A_d attain an extremum on a cirle? Mathematical questions of this kind can be extended and solutions – if found - adapted to arid zone hydrology in the Gulf.

Appendix (Electronic Supplementary File)

In this Appendix, we elaborate on the conformal radius, its definition and some known properties. The conformal radius is a charactersitic of planar domains, which is not well-perceived even by mathematicians. Specifically, in the classical book by Pòlya and Szegö (1951) *R* of domains is considered as a constant that is true if the point z_0 is fixed. Only Bandle and Flucher (1996) and Avkhadiev and Wirth (2009) investigated the properties of *R(x,y)* for various D.

Let D be a simply connected plane domain such that $\infty \notin \mathrm{D}$. Let $z_0 = x + i\, y_0 \in \mathrm{D}$ be a fixed point.

According to the Riemann mapping theorem there exists an analytic function *w=g(z)* that satisfies the conditions $g(z_0) = 0, g'(z_0) = \mathrm{Re}\, g'(z_0) > 0$ and maps conformally the domain D onto the

unit disc D^* =D(0, 0, 1), defined by $|w|<1$ in the *w*-plane.

The function $g(z)/\mathrm{Re}\, g'(z_0)$ maps conformally the domain D onto the disc D(0, 0, *R*) of a radius $R=1/\mathrm{Re}\, g'(z_0)>0$. This positive number, $R(z_0, D)$, is called the conformal radius of the domain D at the point z_0 (see, for example, Pòlya and Szegö, 1951). By this definition, the number *R* is determined for every point z_0 in D. Therefore, the conformal radius is a function, defined at every point $z_0 \in D$ (see, for instance, Bandle and Flucher, 1996, Avkhadiev and Wirths, 2009). Using explicit conformal mappings one easily gets the following known (see e.g. Bandle and Flucher, 1996) formulas

$$R(x+i\,y, D^*)=1-x^2-y^2,\ \ R(x+i\,y, D^{**})=2x,\ \ R(x+i\,y, D^{***})=2\sin x$$

where D^{**} is the half-plane defined by $x>0$, and D^{***} is the strip, defined by $0<x<\pi$.

Of course, in the general case of an arbitrary domain D one has no explicit formulas for conformal radii of domains. Fortunately, there are several useful identities, integral formulas and explicit estimates for the conformal radius of arbitrary simply connected domains.

Consider an arbitrary conformal map by the function $z=f(\zeta)$ of the unit disc onto the domain D. As a simple consequence of the definition of the conformal radius one has the following identity

$$R[f(\zeta), D]\equiv |f'(\zeta)|(1-|\zeta|^2),\quad z=f(\zeta)\in D,\quad \zeta\in D^*=D(0,0,1)$$

Using this formula for a disc of a radius r_0, one easily gets

$$R[z, D(x_0, y_0, r_0)]=r_0-\frac{(x-x_0)^2+(y-y_0)^2}{r_0}$$

We emphasize that the conformal radius is connected with the hyperbolic Lobachevsky geometry in D via the formula $R(z, D)\equiv 1/\lambda_D(z)$, where $\lambda_D(z)$ is the coefficient of the hyperbolic Poincaré metric in D with the Gaussian curvature *c*=-4 (more details see, for instance, in Bandle and

Flucher, 1996, Avkhadiev and Wirths, 2009). This fact, which is not widely known even in the community of mathematicians working with the geometric theory of functions of complex variables, implies many useful consequences. In particular, we have used the Liouville equations and the estimates

$$\frac{1}{4}R(z,\mathrm{D}) \le dist(z,\mathrm{G}) \le R(z,\mathrm{D}), \quad z \in \mathrm{D},$$

which are inferrred from the classical Koebe one-quoter theorem and the Schwarz-Pick inequality (Avkhadiev and Wirth, 2009). It is noteworthy that the Liouville equation in the form

$$R(z,\mathrm{D})\Delta R(z,\mathrm{D}) = |\nabla R(z,\mathrm{D})|^2 - 4, \quad z \in \mathrm{D},$$

where Δ and ∇ are the Laplacian and gradient operators in the (x,y) plane, as well as a conformally invariant version of the Hardy inequality, were the pillars in the analysis of the properties of the moment of inertia I_c with respect to G (Avkhadiev, 1998).

In addition to the described classical properties of the conformal radius of a simply connected domain, we provide below three useful integral formulas, proved by Avkhadiev (2004). Namely, one has the following integral equalities:

$$A(D) = \frac{1}{2}\iint_D |\nabla R(z,D)|^2 \, dxdy,$$
$$\iint_D R^2(z,D)dxdy = \iint_D R^2(z,D)\,|\nabla R(z,D)|^2 \, dxdy,$$

and the inequality

$$2\frac{\left(\iint_D R(z,D)dxdy\right)^2}{A(D)} \le P(D),$$

where equality occurs if and only if D is a disc.

Using the latter inequality and the right side inequality in eqn.(10) we obtain

$$V_w = \iint_{\mathrm{D}} h(x,y)dxdy \le h_0 A(\mathrm{D}) - 2\frac{e\left(\iint_D R(z,\mathrm{D})dxdy\right)^2}{4h_0 A(\mathrm{D})}.$$

where the function *h(x, y)* is defined by the BVP (1)-(2) and $h(x,y) \ge 0$ on the domain D.

Data Availability Statement. We did not use any new data.

Acknowledgments

Avkhadiev was supported by the Russian Science Foundation under the grant no. 18-11-00115. Kacimov was supported by Sultan Qaboos University (SQU) via the grants IG/AGR/SWAE/18/01 and DR/RG/17.

References

+Al-Maktoumi, A., Kacimov, A., Al-Busaidi, H., Al-Ismaily, S., Al-Mayahi, A., Al-Khanbashi, S., and Al-Sulaimi, A., 2020. Enhancement of infiltration rate of clogged porous beds in the vicinity of dams in arid zones by the roots of indigenous *Ziziphus spina-christ* trees. Hydrological Processes (in press).

+Al-Sefry, S.A. and Şen, Z., 2006. Groundwater rise problem and risk evaluation in major cities of arid lands–Jeddah case in Kingdom of Saudi Arabia. Water Resources Management, 20(1), 91-108.

+Al-Senafy, M., Hadi, K., Fadlelmawla, A., Al-Fahad, K., Al-Khalid, and A. Bhandary, H., 2015. Causes of groundwater rise at Al-Qurain residential area, Kuwait. Procedia Environmental Sciences,

25, 4-10.

+ Alsharhan, A. S., and Rizk, Z.E., 2020. Water Resources and Integrated Management of the United Arab Emirates (Vol. 3). Springer Nature, Cham.

+ Al-Shukaili, A., Al- Mayahi, A., Al-Maktoumi, A., and Kacimov, A.R., 2020. Unlined trench as a falling head permeameter: Analytic and HYDRUS2D modeling versus sandbox experiment. J.Hydrology, 583, 124568.

+ Aravin, V.I., and Numerov, S.N., 1953. Theory of motion of liquids and gases in undeformable porous media. Gostechnizdat, Moscow (in Russian), English translation: Israel Program of Scientific Translation, Jerusalem, 1965.

+Arutyunyan, N.Kh., and Abramyan, B.L., 1963. Torsion of Elastic Bodies. Fizmatgiz, Moscow (in Russian).

+Avkhadiev, F. G., 1998. Solution of the generalized Saint Venant problem. Sbornik: Mathematics, 189(12), 1739–1748.

+Avkhadiev, F.G., 2004. New isoperimetric inequalities for moments of domains and torsional rigidity. Russian Mathematics (Izv. VUZ), 48(7), 1-9.

+ Avkhadiev, F. G., 2015. Integral inequalities in hyperbolic-type domains and their application. Sbornik: Mathematics, 206 (12), 1657–1681.

+Avkhadiev, F. G., 2020. Conformally Invariant Inequalities. Kazan, Kazan Federal University (in Russian).

+Avkhadiev, F. G., and Kacimov, A. R., 2002. Analytical solutions and estimates for microlevel flows. J. of Porous Media, 8 (2), 125–148.

+Avkhadiev, F. G., and Wirths, K.-J., 2009. Schwarz-Pick Type Inequalities. Birkhäuser Verlag, Basel.

+Bandle, C., 1980. Isoperimetric Inequalities and Applications. Pitman Monographs and

741 Studies in Mathematics, 7, Boston.

742 +Bandle, C., and Flucher, M., 1996. Harmonic radius and concentration of energy: hyperbolic

743 radius and Liouville's equations $\Delta U = e^U$ *and* $\Delta U = U^{\frac{n+2}{n-2}}$. SIAM Review, 38 (2), 191–238.

744 +Carbery, A., Maz'ya, V., Mitrea, M., and Rule, D., 2014. The integrability of negative

745 powers of the solution of the Saint Venant problem. Ann. Scuola Norm. Super. Pisa-Cl. Sci. 13 (2),

746 465–531.

747 +Garnett, J. B., and Marshall, D. E., 2005. Harmonic Measure. Cambridge Univercity

748 Press, Cambridge.

749 +Coffey, T. S., and Shaw, J. B., 2017. Congruent bifurcation angles in river delta and

750 tributary channel networks. Geophysical Research Letters, 44(22), 11, 427-436.

751 +Cohen, Y., and Rothman, D.H., 2017. Exact solution for the Poisson field in a semi-infinite

752 strip. Proceedings of the Royal Society A: Mathematical, Physical and Engineering Sciences 473,

753 20160908.

754 + Craster, R.V., 1994. Two related free boundary problems. IMA J. of Applied Mathematics,

755 52(3), 253-270.

756 +Haitjema, H. M., 1995. Analytic Element Modeling of Groundwater Flow. Elsevier.

757 +Haitjema, H., 2006. The role of hand calculations in ground water flow modeling.

758 Groundwater, 44(6), 786-791.

759 +Hamutoko, J. T., Post, V. E. A., Wanke, H., Beyer, M., Houben, G., and Mapani, B., 2019.

760 The role of local perched aquifers in regional groundwater recharge in semi-arid environments:

761 evidence from the Cuvelai-Etosha Basin, Namibia. Hydrogeology J., 27(7), 2399-2413.

762 +Healy, R.W., 2010. Estimating Groundwater Recharge. Cambridge University Press.

763 +Hogan, J.E., Phillips, F.M., and Scanlon, B.R. (Editors), 2004. Groundwater Recharge in a

764 Desert Environment: the Southwestern United States. American Geophysical Union.

765 +Hunt, R.J., Prudic, D.E., Walker, J.F. and Anderson, M.P., 2008. Importance of unsaturated
766 zone flow for simulating recharge in a humid climate. Groundwater, 46(4), 551-560.

767 +Kacimov, A.R., 2006. Capillarity and evaporation exacerbated seepage losses from unlined
768 channels. J. Irrigation and Drainage Engineering (ASCE), 132(6), 623-626.

769 +Kacimov, A. , Al-Maktoumi, A., and Šimůnek, J., 2020b. Water table rise in urban
770 shallow aquifer with vertically-heterogeneous soils: Girinskii's potential revisited. Hydrological
771 Sciences J. (in press).

772 +Kacimov, A.R., Obnosov, Yu.V., and Perret, J., 2004. Phreatic surface flow from a
773 near-reservoir saturated tongue. J. Hydrology, 296, 271-281.

774 +Kacimov, A.R. and Obnosov, Yu.V., 2006. Strip-focused phreatic surface flow driven by
775 evaporation: analytical solution by the Riesenkampf function. Advances in Water Resources, 29,
776 1565-1571.

777 +Kacimov, A.R., Obnosov, Yu.V., Sherif, M.M., and Perret, J., 2006. Analytical solution to a
778 sea water intrusion problem with a fresh water zone tapering to a triple point. J. Engineering
779 Mathematics, 54(3), 197-210.

780 +Kacimov, A.R., Sherif, M.M., Perret, J.S., and Al-Mushikhi, A., 2009. Control of sea-water
781 intrusion by salt-water pumping: Coast of Oman. Hydrogeology J., 17, 541-558

782 +Kacimov, A., Kayumov, I., and Al-Maktoumi, A., 2016. Rainfall induced groundwater
783 mound in wedge-shaped promontories: the Strack-Chernyshov model revisited. Advances in Water
784 Resources, 97, 110-119.

785 +Kacimov, A.R., Maklakov, D.V., Kayumov, I.R., and Al-Futaisi, A., 2017a. Free surface
786 flow in a microfluidic corner and in an unconfined aquifer with accretion: the Signorini and
787 Saint-Venant analytical techniques revisited. Transport in Porous Media, 116(1), 115-142.

+Kacimov, A.R. and Obnosov, Yu.V., 2006. Strip-focused phreatic surface flow driven by evaporation: analytical solution by the Riesenkampf function. Advances in Water Resources, 29, 1565-1571.

+Kacimov, A., Obnosov, Yu., and Al-Maktoumi, A., 2017b. Phreatic/confined flows in polygons: Dupuit-Forchheimer model versus potential solutions. European Water, 57, 489-496.

+Kacimov, A., Obnosov ,Yu.V., and Simunek, J., 2018. Steady flow from an array of subsurface emitters: Kornev's irrigation technology and Kidder's free boundary problems revisited. Transport in Porous Media. 121(3), 643-664.

+Kacimov, A., and Obnosov, Yu.V., 2019. Analytic solutions for infiltration-evaporation formed fresh groundwater lenses floating on saline water table under desert dunes: Kunin-Van Der Veer legacy revisited. J. Hydrology, 574, 733-743.

+Kacimov, A., Obnosov, Yu.V., and Or, D., 2019. Evaporation induced capillary siphoning through hydraulically connected porous domains: the Vedernikov-Bouwer model revisited. Transport in Porous Media, 129 (1), 231–251.

+Kacimov, A.R., and Youngs, E.G., 2005. Steady-state water-table depressions caused by evaporation in lands overlying a water-bearing substratum. J. Hydrologic Engineering (ASCE), 10(4), 295-301.

+Kacimov, A., Yakimov, N.D., and Šimůnek, J. , 2020a. Phreatic seepage flow through an earth dam with an impeding strip. Computational Geosciences, 24, 17–35.

+Keady, G., and Wiwatanapataphee, B., 2020. Variational approximations for steady unidirectional slip flows in microchannels. J.of Fluids Engineering, 142(7), 074501-1 - 074501-3.

+Kreibich, H., and Thieken, A.H., 2008. Assessment of damage caused by high groundwater inundation. Water Resources Research, 44, W09409.

+Mahdavi, A., 2020. Steady-state response of annular wedge-shaped aquifers to

arbitrarily-located multiwells with regional flow. J. Hydrology, p.124906.

+McDonald, N.R., 2020. Finger growth and selection in a Poisson field. J. of Statistical Physics, 178(3), 763-774.

+Minnig, M., Moeck, C., Radny, D., and Schirmer, M., 2018. Impact of urbanization on groundwater recharge rates in Dübendorf, Switzerland. J. of Hydrology, 563, 1135–1146.

+Moeck, C., von Freyberg, J., and Schirmer, M., 2018. Groundwater recharge predictions in contrasted climate: The effect of model complexity and calibration period on recharge rates. Environmental Modelling & Software, 103, 74-89.

+Niswonger, R.G., and Fogg, G.E., 2008. Influence of perched groundwater on base flow. Water Resources Research, 44.3.

+Philip, J. R.,1991. Upper bounds on evaporation losses from buried sources. Soil Science Society of America J., 55(6), 1516-1520.

+Polubarinova-Kochina, P.Ya., 1962. Theory of Ground Water Movement. Princeton University Press, Princeton. The second edition of the book (in Russian) was published in 1977, Nauka, Moscow.

+Pòlya, G., and Szegö, G., 1951. Isoperimetric inequalities in mathematical physics. Ann. of Math. Stud., 27, Princeton Univ. Press, Princeton, N. J.

+ Rezaei, M., De Pue, J., Seuntjens, P., Joris, I., and Cornelis, W., 2017. Quasi 3D modelling of vadose zone soil-water flow for optimizing irrigation strategies: Challenges, uncertainties and efficiencies. Environmental Modelling & Software, 93, 59-77.

+de Saint-Venant, B., 1856. Mémoire sur la torsion des prismes. Mémoire présentés par divers savants á l'Académie des Sciences, 14, 233–560 (in French).

+Salahudinov, R. G., 2001. Isoperimetric inequality for torsional rigidity in the complex plane. J. of Inequalities and Applications, 6 (4), 253–260.

+Sasidharan, S., Bradford, A., Šimůnek, J., DeJong, B., and Kraemer, S.R., 2018. Evaluating drywells for stormwater management and enhanced aquifer recharge. Advances in Water Resources, 116, 167-177.

+Silliman, S. E., Berkowitz, B., Šimůnek, J., and van Genuchten, M. Th. , 2002. Fluid flow and solute migration within the capillary fringe. Ground Water, 40(1), 76-84.

+Šimůnek, J., van Genuchten, M. Th., and Šejna, M., 2016. Recent developments and applications of the HYDRUS computer software packages. Vadose Zone J., 15(7), pp. 25, doi: 10.2136/vzj2016.04.0033.

+Shokri-Kuehni, S.M., Raaijmakers, B., Kurz, T., Or, D., Helmig, R. and Shokri, N., 2020. Water table depth and soil salinization: From pore-scale processes to field-scale responses. Water Resources Research, 56(2), p.e2019WR026707.

+Strack, O.D., 2017a. Analytical Groundwater Mechanics. Cambridge University Press.

+Strack, O.D., 2017b. Vertically integrated flow in stratified aquifers. J. of Hydrology, 548, 794-800.

+Strack, O.D.L., 2020. Applications of Vector Analysis and Complex Variables in Engineering. Springer, Cham.

+Toller, E.A., and Strack, O.D., 2019. Interface flow with vertically varying hydraulic conductivity. Water Resources Research, 55(11), 8514-8525.

+ Timoshenko, S. R., 1954. History of the Strength of Materials. McGraw-Hill, London.

+Villeneuve, S., Cook, P.G., Shanafield, M., Wood, C., and White, N., 2015. Groundwater recharge via infiltration through an ephemeral riverbed, central Australia. J. of Arid Environments 117, 47-58.

+Wolfram, S., 1991. *Mathematica.* A System for Doing Mathematics by Computer. Addison-Wesley, Redwood City.

+Youngs, E.G., 1990. An examination of computed steady-state water-table heights in unconfined aquifers: Dupuit-Forchheimer estimates and exact analytical results. J. Hydrology, 119(1-4), 201-214.

+Zhang, Y., Wang, X., Liu, D., Yi, Y., Li, C., Liu, Q., and Cai, Y., 2020. An improved model for investigating dual effects of vegetation density variations and groundwater level fluctuations on water transport and dissipation in raised field wetlands. Wetlands, 1-16. https://doi.org/10.1007/s13157-020-01277-6

+Zijl, W., De Smedt, F., El-Rawy, M., and Batelaan, O., 2017. The Double Constraint Inversion Methodology: Equations and Applications in Forward and Inverse Modeling of Groundwater Flow. Springer.

List of Acronyms

BVP=Boundary value problem

DF =Dupuit-Forchhemier

PDE=Partial differential equation

PK-62=reference to Polubarinova-Kochina (1962)

VG=Van Genuchten

Figures Legends

Fig. 1. Plan (aerial) view of an unconfined aquifer.

Fig.2. Vertical cross-sections. Unconfined aquifer with: no unsaturated lacunae a), one lacuna b), two lacunae c).

Fig.3. HYDRUS simulations for saturated-unsaturated axisymmetric flow in a circular cylinder

883 at *t*=600 days: a) phreatic surface TB for |AB|=50 cm.; b) isohumes $\theta(x,Z)$; c) vectors of Darcian
884 velocities; d) streamlines; e) phreatic surface with concave-up and concave-down segments for
885 |AB|=75 cm.

886 Fig.4. HYDRUS simulations for a cylinder having r_0=20 m at *t*=600 days: a) phreatic surface TB
887 for |AB|=50 cm.; b) isohumes; c) Darcian velocities near AC; d) velocity magnitude along CD(left
888 panel) and evaporation rate *e(Z)* computed in Wolfram's (1991) *Mathematica* (right panel); e)
889 velocity along AB.

890